International Journal of Applied Engineering Research ISSN 0973-4562 Volume 12, Number 14 (2017) pp. 4415-4421

CFD Analysis of a Flat Plate Solar Collector for Improvement in Thermal Performance with Geometric Treatment of Absorber Tube

K. Vasudeva Karanth[1] and Jodel A. Q. Cornelio

[1]*Department of Mechanical & Mfg. Engineering, Manipal Institute of Technology, Manipal University, Manipal 576104, Karnataka, India.*

[2]*Department of Mechanical & Mfg. Engineering, Manipal Institute of Technology, Manipal University, Manipal 576104, Karnataka, India.*

[1]ORCID: 0000-0001-6138-1204

Abstract

It is generally found that energy utilization in the residential and industrial applications of water heating systems is now a days developed by solar collectors. Even though there are solar water heaters with different configuration, they are constructed with absorber tubes having circular cross section. This study analyzes the implications on thermal performance when different sizes and shapes are adopted for the tubes of absorber plate. It is seen from the CFD analysis that the circular cross section tube of the collector having flattened out contact surface with that of the absorber plate provides significantly better thermal performance vis-à-vis other configurations in terms of Nusselt number. The comparison criteria adopted were constant area of cross section along flow path and constant perimeter of the tube flow path for different designs adopted in the analysis. Criterion with constant cross section area showed that the pressure drop and absolute temperature rise across the tube were relatively large for triangular tube design. For the criterion with constant perimeter interestingly, geometry with rectangular cross section provided the highest temperature rise while for the configuration with trapezium cross section, highest drop in the pressure was inferred. This study enables us to develop a prescription for design of size and shape of cross section of various absorber tubes.

Keywords: Solar water heater, radiation, heat transfer, solar collector, computational fluid dynamics. Introduction (Heading 1)

INTRODUCTION

Heating of water for industrial and domestic applications is largely being done using solar collectors these days. There are large number of configurations of solar water heaters in commercial use and are invariably made up of water tubes having circular cross section. There is a need to assess the performance of solar collector with a view to improve its performance so that the contribution to the world in terms of energy savings will be significant..

Gertzos and Caouris, [1] carried out a 3D CFD-study of solar water heater by adopting standard k–ω model for simulating turbulence. Their study also validated the CFD model and achieved good agreement with the experimental results. Varol and Oztop [2] numerically studied the natural heat transfer due to convection inside an inclined solar wavy collector and solar flat-plate collector. They observed that flow and thermal fields were affected by the shape of enclosure and heat transfer rate increased in the case of wavy enclosure than that of flat enclosure. Selmi et al. [3] in their study, Validated the CFD simulated results of solar flat plate collector. The study of the collector thermal performance was carried out with and without water circulating flow conditions. The outlet temperature of water which was compared with the experimental results was found to be having good agreement. Ho et al. [4] carried out theoretical study and experimented with "recyclic" solar flat plate water heater containing rectangle conduits. They found that under the given absorber area and a distance between the flow conduits, the efficiency of the collector decreased with decreased aspect ratio of flow condition, but with increase inlet water temperature.

Michele et al. [5] analyzed the characteristics of solar water heater with water In glass evacuated tube along with calculation of the circulation rate through single ended tubes. They found that heat distribution along the circumference was an influential parameter that effected circulation rate and flow structure through the tube. Aaron et al. [6] carried out a combined conductive, convective and radiative, heat transfer analysis of solar water heaters. The spectral distribution of the irradiance caused by solar radiation was adopted in the study to account for radiation effects. The model which was developed was used to predict temperatures and heat flux for a solar flat-plate collector for geometrical variations and flow conditions.

A comprehensive model to carry out a preliminary design of flat plate solar collectors was developed by Mauricio et al. [7] with the adoption of phase changing material technology and analyzed various configurations. Debayan et al. [8] analyzed solar heaters undergoing discrete distributed natural

convection in the triangular and square cavities with the help of computational fluid dynamics and heat line simulations. They showed that there was an improvement in the efficiency of mixing for the inverted triangular and square enclosures provided in a solar heater, with respect to discrete solar heaters. The flow and heat transfer performance of solar water heaters for different initial temperatures with elliptical collector tubes were evaluated by Kaichun et al. [9] using numerical simulation. It was found that there was no change in the temperature profile for all cross sections of the tube. However, the velocity profiles were not similar. It was also found that the flow velocity saw a decrement near to the wall of the tube as the ratio of the major and minor axis of elliptical cross section decreased and thus producing the reduction in the rate of circulation throughout the collector tubes and hence was not suitable for convective heat transfer. It was observed that the solar water heater with elliptical cross section had a lower Nusselt number when compared to that of the circular cross section solar water heater.

From the above literature it can be observed that a study to analyze the thermal performance of solar collector with different geometry for absorber tube was required to understand the heat transfer phenomena in all these designs. Hence a numerical study using the Ansys Fluent software is carried out to find the efficacy of solar water heater with different geometry and shapes for absorber tubes.

NUMERICAL MODELING

A. Base model geometric configuration

For the study of solar water heater, a circular cross section water tube of half an inch outer diameter and 1.2 meter length is adopted. The vertical dimension from the centerline of the collector and the bottom surface of absorber plate is taken as 0.003 m. The copper absorber tube thickness is 0.65 mm. A copper absorber plate of 0.5 mm thickness, 0.15 m width, and 1.2 m length is attached above the absorber tube with a small angle of lap. The center line of the collector passes through the absorber tube.

B. Criteria adopted for comparison

For evaluating the thermal performance of configurations with different shapes for cross section (refer Fig 1), two distinct criteria's are adopted which influence the Nusselt number. They are i) Constant area criteria and ii) constant perimeter criteria for the absorber tube and the magnitudes of the same for different geometry's are as shown in tables 1 and 2. The glass cover above the absorber plate is 5 mm thick and has an air gap of 10 mm between them. The bottom surface of the absorber plate and absorber tube is insulated and an adiabatic condition is adopted in the numerical study.

It can be noted that the circular cross section tube has an arc shaped angle of lap with that of the absorber plate whereas for all other configurations the surface area of contact with absorber plate is flat. For the purpose of comparison, the constant area and perimeter corresponds to the circular cross section water tube in tables 1 and 2.

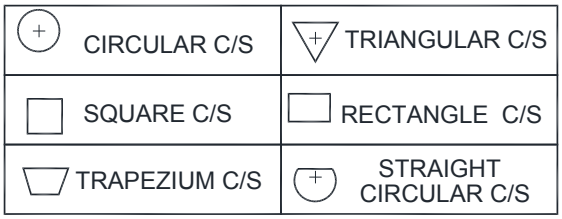

Figure 1: Shape of cross section of absorber tube adopted in the study

TABLE 1: PERIMETER AND HYDRAULIC DIAMETER FOR CONFIGURATIONS WITH A CONSTANT FLOW AREA

Shape	Perimeter (mm)	Hydraulic diameter (mm)
Circle	32.3584	10.29999011
Square	36.5125	9.128139678
Triangle	41.6151	8.008900615
Rectangle	37.70976	8.838327266
Trapezium	37.470854	8.894678515
Straight Circle	33.52531	9.941480034

TABLE 2. AREA AND HYDRAULIC DIAMETERS FOR CONFIGURATIONS WITH A CONSTANT PERIMETER

Shape for cross section	Area of Cross section (mm^2)	Hydraulic diameter (mm)
Circle	83.323	10.29999011
Square	65.442	8.089596519
Triangle	50.377	6.227328916
Rectangle	61.352	7.584
Trapezium	46.867	5.793537381
Straight Circle	77.694	9.604146064

A grid independence test is carried out for the circular cross section tube with 1.4, 1.8, 2.0, 2.4, 2.8, and 3.2 million elements. It is observed that for configuration having 2.4 million elements or above, the change in temperature is not more than 0.5 % and therefore to conserve computational time, the configuration with 2.4 million elements is adopted. The meshed domain is made up of water, absorber tube, absorber plate, air gap and the glass cover together made up of

2.4 million hexahedral elements. A localized view of the meshed domain is shown in figure 2.

Discrete Ordinate (DO) radiation model is adopted to simulate the solar ray tracking condition. The latitude and longitude values of Manipal are input in the calculation according to the data obtained from Google Maps for the location where the experimental work is carried out. The time and day of the experimentation is input in the solar ray tracking calculation.

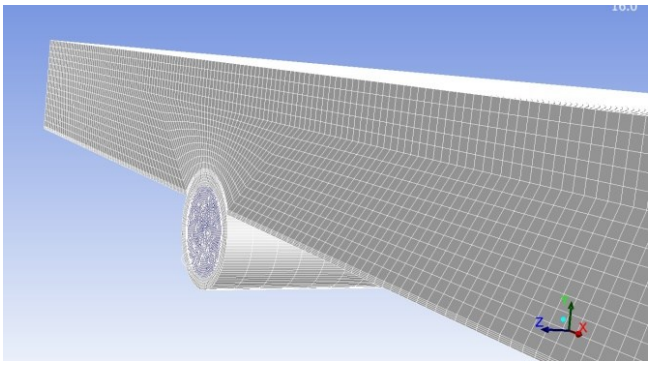

Figure 2: An enlarged portion of the domain control volume

The solar radiation inputs adopted in the study areas flows.

Sun direction vector: X = -0.0650444, Y = 0.860404,

Z = 0.505444.

Diffuse solar irradiation – vertical surface: 52.0175.

Diffuse solar irradiation – horizontal surface: 60.9133.

Ground reflected solar irradiation: 95.3581.

The material properties of air, copper, glass and water adopted are tabulated as shown in Table 3.

Polynomial coefficient values for air within the air gap are as follows

Thermal Conductivity: a = 1.5121e-06, b = 9.7459e-05,

c = -3.3322e-08.

Viscosity: a = 1.6157e-06, b = 6.523e-08, c = -3.0297e-11.

Density: a = 3.9147, b = -0.01682, c = 2.9013e-05,

d = 1.9407e-08.

Standard k-epsilon model is adopted to take into account the turbulent conditions that might occur in the flow domain. Turbulent intensity of 5% is provided at the inlet.

C. Mean Flow Equations:

Analysis is carried out for steady state conditions by solving the partial differential governing equations of mass and momentum. The equations of continuity, momentum and energy are presented as shown in equations (1), (2) and (3) and are given in the "Cartesian tensor notation".

Equation of Continuity is given as:

$$\frac{\partial}{\partial x_i}(\rho U_i) = 0 \tag{1}$$

Equation of Momentum is given as,

$$\frac{\partial}{\partial x_j}(\rho U_i U_j) = \frac{\partial P}{\partial x_i} + \frac{\partial}{\partial x_j}\left[\mu\left(\frac{\partial U_i}{\partial x_j} + \frac{\partial U_j}{\partial x_i}\right) - \rho\overline{u_i u_j}\right] \tag{2}$$

Equation of Energy is given as,

$$\frac{\partial}{\partial x_j}(\rho U_i T) = \frac{\partial}{\partial x_j}\left[\frac{\mu}{\Pr}\frac{\partial T}{\partial x_j} - \rho\overline{u_i t}\right] \tag{3}$$

TABLE 3: PROPERTIES OF MATERIAL USED IN THE COLLECTOR DESIGN

Material	Thermal conductivity (W/mK)	Specific Heat (kJ/kg-K)	Refractive Index	Viscosity (m^2/s^2)	Density (kg/m^3)
Air	Polynomial	1.006	1.0	Polynomial	Polynomial
Copper	387.6	381	-	-	8978
Glass	1.14	831	1.5	-	2230
Water	0.6	4.182	1.0	0.658e-6	998.2

The pressure-velocity coupling is carried out using the SIMPLE algorithm of Patankar [10]. Discretisation is done using the second order upwind scheme. The momentum and energy continuity equations are solved until the residual values of 1e-06 are achieved.

D. Validation of numerical results

The validation of numerical results of circular cross section tube solar flat plate collector with experimental results is carried out for 5 different mass flow rates and the temperature rise coefficient vs. Reynolds number is shown in figure 3. The temperature rise coefficient across the tube is calculated using eq(4).

$$C_t = \frac{T_o - T_i}{T_i} = 0 \tag{4}$$

Where T_o is the outlet temperature and T_i is the temperature of water at inlet. It can be noted from figure 3 that there exists some difference between the numerical and experimental results. However the trends of the two curves are in agreement with each other. The gap between the numerical results and experimental results can be for the reason that the numerical analysis adopts perfect insulating conditions and complete heat transfer from the absorber plate to the absorber fluid unlike the experimental results.

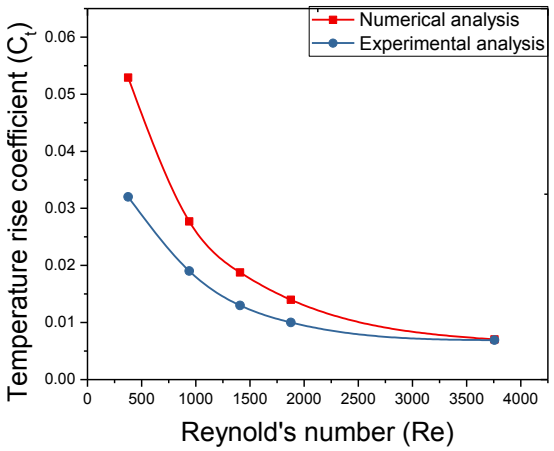

Figure 3: Validation curves of numerical results with that of experimental results

RESULTS AND DISCUSSION

The numerical study of various configurations are carried out by adopting constant area of flow criteria and constant perimeter criteria and figures 4 and 5 show the plots of Nusselt number in terms of their area weighted average values. It can be observed from these bar diagrams that the Nusselt number of configuration with circular cross section absorber tube having straight contact surface with absorber plate (straight circle) gives the maximum Nusselt number for both the criteria's. This could be attributed to the fact that the radiation heat gets absorbed uniformly by the flat surface of contact with the absorber plate and the circular cross section helps to produce maximum heat transfer to the fluid. However from heat transfer coefficient point of view it can be seen that even though the constant area criteria shows that the maximum heat transfer is for the circular straight cross section configuration (Fig 6), the constant perimeter criteria shows that the trapezium configuration provides the maximum possible heat transfer (Fig. 7). This could be attributed to the reason that the trapezium shpe has the largest contact surface area with the absorber plate.

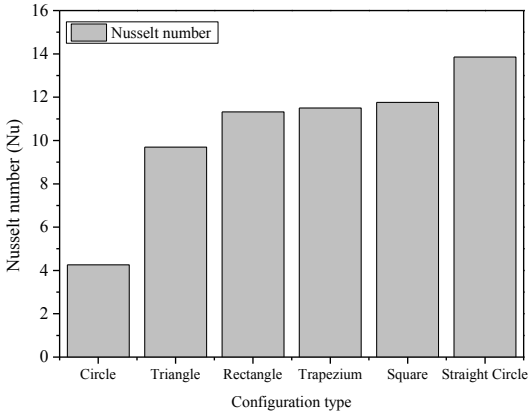

Figure 4: Nusselt number of configurations with constant area criteria

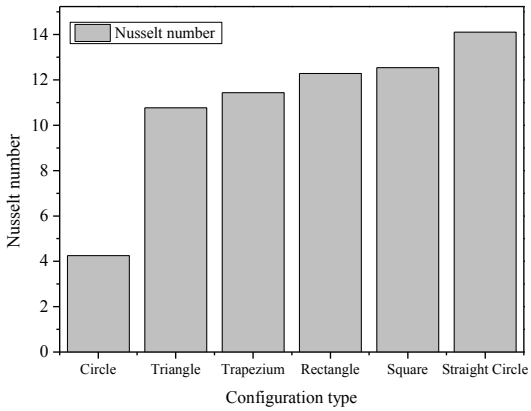

Figure 5: Nusselt number of configurations with constant perimeter criteria

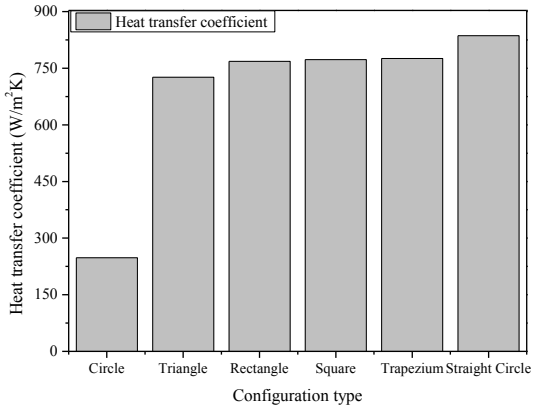

Figure 6: Heat transfer coefficient for configurations with constant area criteria

Referring to figure 8 we can observe that the average temperature rise across the absorber tube is maximum for configuration with triangular cross section, when constant area criteria is adopted. The reason for this can be attributed to the temperature profile of fluid across the triangle cross

section tube which shows a large temperature gradient throughout its periphery (Fig. 16) and has the largest perimeter (see table 1).

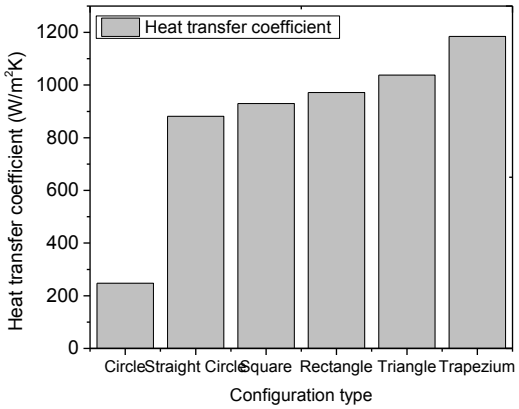

Figure 7: Heat transfer coefficient of configurations with constant perimeter criteria

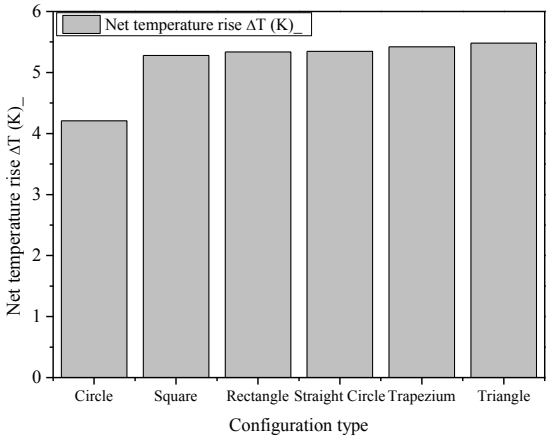

Figure 8: Net temperature rise across the tube for configurations with constant area criteria

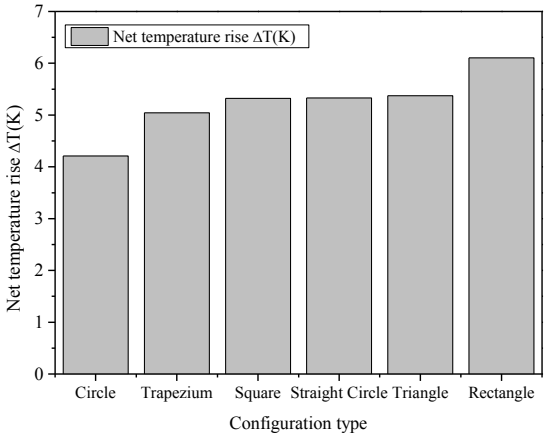

Figure 9: Net temperature rise across the tube for configurations with constant perimeter criteria

The temperature rise across the tube is maximum for configuration with rectangle cross section when constant perimeter criterion is adopted (fig. 9). The reason for this can be due to the fact that uniform heating takes place across the width of the rectangle with reference to its height compared to all other configurations.

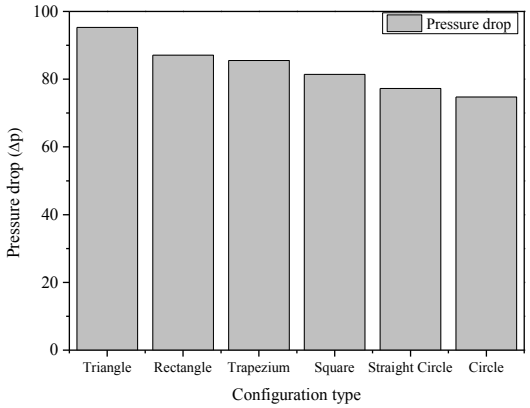

Figure 10: Pressure drop across the tube for configurations with constant area criteria

Referring to fig. 10, the maximum pressure drop across the absorber tube is found to be for triangular configuration when 'constant area criteria' is adopted. This can be due to the reason that the sharp corners of the tube tend to offer resistance to the flow. Also the triangular cross section tube has the largest perimeter and hence has the largest area of wall surface, leading to large resistance.

For the constant perimeter criteria adopted in the study it is noted from fig. 11 tht the largest pressure drop is for the trapezium cross section configuration followed by triangular cross section configuration. This can be explained with the reasoning that same mass flow rate is applied across all the configurations and the mass flow rate is a product of density, area and velocity. From table 2 it can be noted that the trapezium cross section has the lowest area of cross section followed by triangular cross section and hence to keep the mass flow rate constant, the velocity for trapezium and triangular cross sections increases proportionately and hence leading to larger pressure loss across the tube.

Figures 12 to 17 show the temperature profile across the water heater near to the exit of the collector for various configurations. The plots show how the radiation heat gets concentrated towards the water tube and the heat flow pattern across the air gap between the absorber plate and the glass cover.

A comparative temperature plot for various configurations is shown in figure 18. The plot of temperature is captured along the central flow path for each of the configurations. It can be observed that the temperature gradients are very steep for

configurations other than circular and straight circular cross section in the initial stage. The initial transients and the large gap can be due to the reason that the fluid that enters the absorber tube gains heat as it progresses through the flow path. However for circular and straight circular cross section configurations, the laminar flow pattern does not get disturbed unlike the other configurations and the distance from the center line to the absorber plate is larger than that of the other configurations.

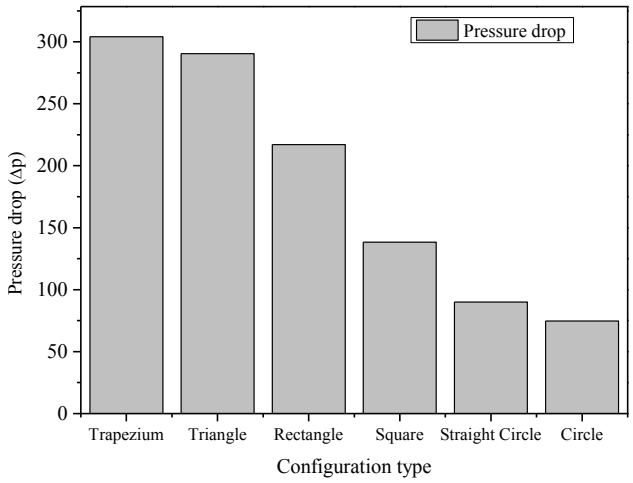

Figure 11: Pressure drop across the tube for configurations with constant perimeter criteria

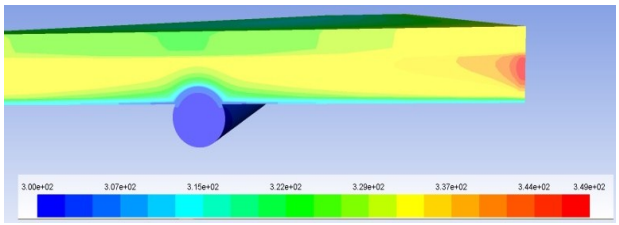

Figure 12: Cut across temperature plot near the exit of the circular cross section configuration

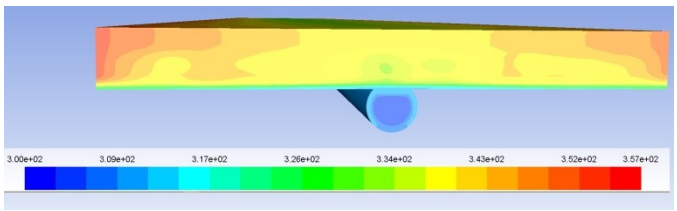

Figure 13: Cut across temperature plot near the exit of the straight circule configuration

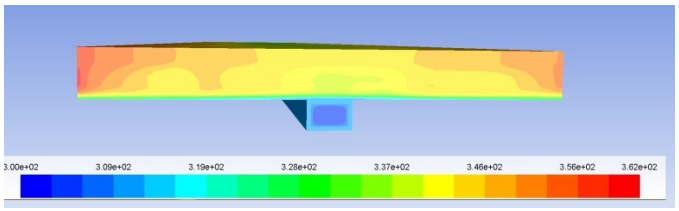

Figure 14: Cut across temperature plot near the exit of the rectang configuration

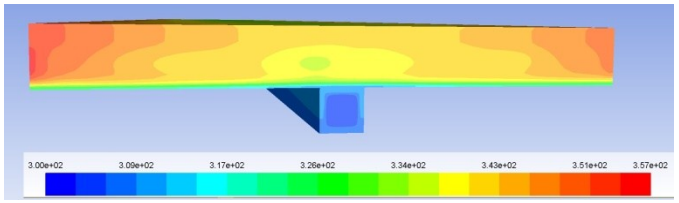

Fig. 15, Cut across temperature plot near the exit of the square configuration

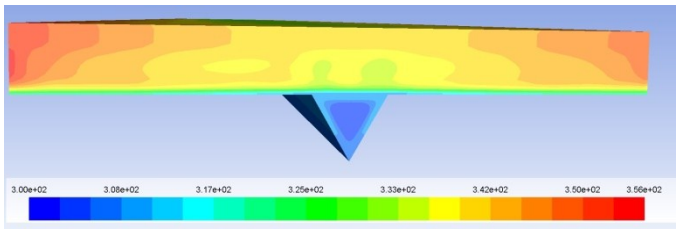

Fig. 16, Cut across temperature plot near the exit of the triangle configuration

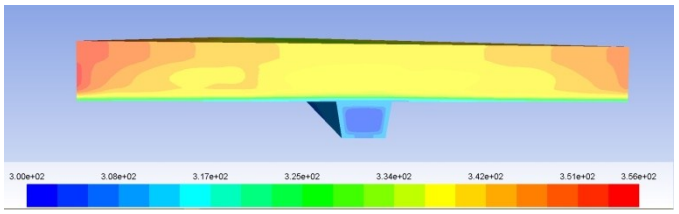

Fig. 17, Cut across temperature plot near the exit of the trepazium configuration

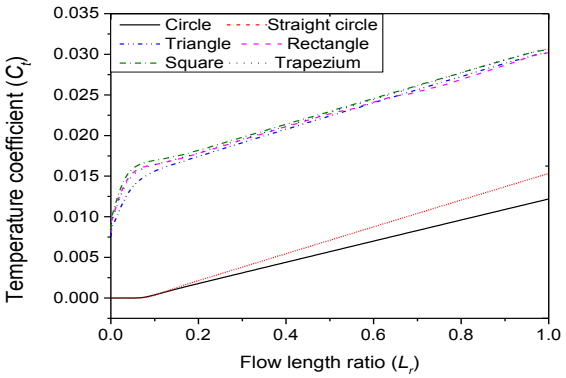

Figure 18: Temperature plots along the flow length at the center of the absorber tube for configurations with constant area criteria

CONCLUSION

The numerical study shows that the thermal performance variations are significant while different shapes and size are considered for the solar collector tubes based on the criteria's of constant area of cross section and constant perimeter. The following conclusions are drawn from the study.

- The circular cross section tube of the collector having flattened out contact surface with that of the absorber plate provides significantly better thermal performance vis-à-vis other configurations in terms of Nusselt number.
- Criterion with constant cross section area shows that the pressure drop and absolute temperature rise across the tube is relatively large for triangular tube design.
- For criteria based on constant perimeter of crosse section of water tube, configuration with rectangular cross section provides the maximum temperature rise across the tube whereas for the configuration with trapezium cross section absorber tube, pressure drop is observed to be the largest.

NOMENCLATURE

Re	Reynolds number
T	Temperature (^oC)
U	Velocity (m/s)
k	Thermal conductivity (W/m^oC)
ρ	Density (kg/m^3)
μ	Viscosity (Ns/m^2)
Pr	Prandtl number
C_T	Temperature rise coefficient
L_r	Length ratio (L_x/L)

ACKNOWLEDGMENT

The authors are thankful to Manipal University for all the computational facility that is provided for carrying out the numerical study.

REFERENCES

[1] Gertzos, K.P., Caouris, Y.G., "Experimental and computational study of the developed flow field in a flat plate integrated collector storage (ICS) solar device with recirculation". Experimental Thermal and Fluid Science, Vol. 31, pp. 1133 - 1145, 2007.

[2] Varol, Y., Oztop, H.F., "Buoyancy induced heat transfer and fluid flow inside a tilted wavy solar collector", Building and Environment, Vol. 42, pp. 2062 - 2071, 2007.

[3] Selmi M., Al-Khawaja, M.J., Marafia, A., "Validation of CFD simulation for flat plate solar energy collector". Renewable Energy, Vol. 33, pp. 383 - 387, 2008.

[4] Ho, C., Chen, T., and Tsai, C., "Experimental and theoretical studies of re-cyclic flat-plate solar water heaters equipped with rectangle conduits", Renewable Energy, Vol. 35 (10), pp. 2279 - 2287, 2010.

[5] Michele Pinelli, Alessio Suman, Michele Vanti, "Numerical Simulation of Evacuated Tube Solar Water Heaters", ASME Proceedings |, Concentrating Solar Power Plants, vol. 6, pp. 325 -335, June 11 2012.

[6] Aaron P. E., "Mohammad H.N. Combined Convective-Radiative Thermal Analysis of a Solar Flat-Plate Collector", ASME Proceedings |, Advanced Energy Systems: Wind, Solar and Geothermal ASME 56604, pp.. 1 – 7, June 28, 2015.

[7] Mauricio C., Gabriel C., Humberto G. V., Antonio B., "Reduced Model for a Thermal Analysis of a Flat Plate Solar Collector With Thermal Energy Storage Using Phase Change Material (PCM)", ASME 57441, Volume 6B, Nov13 2015.

[8] Debayan D., Tanmay B., "Role of distributed/discrete solar heaters during natural convection in the square and triangular cavities: CFD and heatline simulations", Journal of Solar Energy, Vol. 135, pp. 130 - 153, October 2016.

[9] Kaichun Li, T. Li, H. Tao, Y. Pan, J. Zgang, "Numerical investigation of flow and heat transfer performance of solar water heater with elliptical collector tube", Energy Procedia, Volume 70, pp. 285-292, 2016.

[10] Patankar S.V., "Numerical heat transfer and fluid flow", 1st edition, Hemisphere Publishing Company., Minnesota USA, 1980.